Avicenna Journal of Phytomedicine (AJP)

Original Research Article

Pterostilbene exhibits anti-amoebic and anti-virulence activities against *Entamoeba histolytica* through oxidative stress induction and suppression of virulence-associated genes

Hussam Saeed Al-Aredhi[1,*]

[1]*Department of Biology, College of Education, University of Al-Qadisiyah, Iraq*

Article history:
Received: Jul 11, 2026
Received in revised form: Aug 21, 2026
Accepted: Aug 23, 2026
Epub ahead of print

**** Corresponding Author:***
hussam.saeed@qu.edu.iq

Keywords:
Natural products
Amoebiasis
Oxidative stress
Virulence
Cytotoxicity

Abstract

Objective: This study evaluated the anti-amoebic, anti-virulence, and cytotoxic effects of pterostilbene (PS), alone and combined with metronidazole (MZ), against *Entamoeba histolytica* trophozoites.

Materials and Methods: Trophozoite viability was quantified using the WST-1 assay, and synergistic interactions between agents were assessed via the fractional inhibitory concentration index (FICI). Cytotoxicity was evaluated in FHC intestinal epithelial cells, with selectivity indices calculated. Intracellular reactive oxygen species (ROS) generation was measured using the DCFH-DA assay, and qPCR analyzed expression of key virulence genes (*EhCP1*, *EhCP5*, and *hgl*). Trophozoite adhesion capacity was also examined.

Results: PS significantly reduced trophozoite viability dose-dependently, with IC_{50} values of 37.1 µM for PS, 28.6 µM for MZ, and 12.7 µM for the combination. A pronounced synergistic effect was observed, with FICI ranging from 0.342 to 0.444. Selectivity indices were 10.71 for PS, 10.18 for MZ, and 14.14 for the combination. ROS levels rose 1.79-fold with PS and 3.62-fold with combination therapy. Virulence gene expression was significantly downregulated, particularly in the combination group, with relative levels of 0.21 (*EhCP1*), 0.16 (*EhCP5*), and 0.19 (*hgl*). Adhesion decreased significantly to 44.6% and 22.7% with PS alone and the combination, respectively.

Conclusion: PS exhibits anti-amoebic activity against *E. histolytica* and enhances MZ efficacy under experimental conditions. These effects were associated with increased intracellular ROS, reduced expression of virulence-related genes, and impaired parasite adhesion. Although altered redox homeostasis may contribute to these effects, further in vivo and mechanistic studies are required to confirm PS therapeutic potential.

Please cite this paper as:
Al-Aredhi H.S. Pterostilbene exhibits anti-amoebic and anti-virulence activities against Entamoeba histolytica through oxidative stress induction and suppression of virulence-associated genes. Avicenna J Phytomed, 2026

Introduction

Amoebiasis, an intestinal infection caused by the protozoan parasite *Entamoeba histolytica*, continues to pose a significant clinical and public health concern, particularly in low- and middle-income countries (Danish et al. 2023). The primary mode of transmission is fecal–oral, occurring through the ingestion of mature cysts present in contaminated water, food, or fomites, as well as via direct person-to-person contact in environments with poor sanitation. Upon excystation in the small intestine, trophozoites colonize the large intestine where they may either remain asymptomatic or invade the colonic mucosa, resulting in clinical manifestations (Nasrallah et al. 2022). Although global epidemiological data estimate that approximately 50 to 100 million individuals are infected annually, leading to an estimated 70,000 to 100,000 deaths each year, the actual disease burden is likely underestimated due to diagnostic challenges and frequent misidentification with morphologically indistinguishable non-pathogenic species such as *E. dispar* (Nasrallah et al. 2022; Suleiman and Azlan 2025).

The pathogenic process of *E. histolytica* is orchestrated by a precisely regulated array of virulence factors that facilitate adhesion, cytolysis, and tissue invasion (Guillén 2023). Notably, the *Gal/GalNAc* lectin complex is critical for the parasite's attachment to intestinal epithelial cells and mucus layers, constituting the initial and indispensable step in colonization. Following this, cysteine proteases, especially *EhCP1* and *EhCP5*, are pivotal in degrading extracellular matrix components, compromising epithelial barriers, and modulating host immune responses (Samie et al. 2012). Recent transcriptomic and functional analyses have demonstrated a strong correlation between the upregulation of these virulence genes and invasive disease phenotypes (Samie et al. 2012).

Despite significant progress in the field of molecular parasitology, existing therapeutic approaches for amoebiasis remain constrained (Morán et al. 2023). The primary treatment modality involves the use of nitroimidazole agents, notably metronidazole (MZ), which demonstrate efficacy against the trophozoite stage of the parasite. However, these compounds present several notable limitations including adverse gastrointestinal and neurological effects, limited efficacy against cystic forms, and emerging concerns regarding decreased susceptibility in certain clinical scenarios (Morán et al. 2023). These challenges underscore the critical need to develop alternative anti-amoebic interventions, with an emphasis on targeting parasite virulence factors rather than exclusively focusing on parasite viability.

In recent years, there has been a growing interest in natural products and plant-derived polyphenols as potential anti-parasitic agents, attributed to their multi-target biological activities, favorable safety profiles, and capacity to modulate host–pathogen interactions (Alnomasy et al. 2021; Chaachouay and Zidane 2024). Pterostilbene (trans-3,5-dimethoxy-4-hydroxystilbene, PS) is a naturally occurring dimethylated analog of resveratrol, which is present in blueberries, grapes, and various other berries. PS has gained attention as a promising candidate due to its superior lipophilicity, enhanced bioavailability, and greater stability relative to structurally related stilbenes (Estrela et al. 2013). PS has exhibited anti-inflammatory, antioxidant, and antimicrobial effects across various biological systems (Estrela et al. 2013; Kosuru et al 2016; Obrador et al. 2021). Nonetheless, despite these encouraging biological properties, the anti-amoebic potential of PS remains inadequately explored, and its influence on the molecular determinants of *E. histolytica* virulence has yet to be comprehensively characterized. Furthermore, although prior investigations

have assessed plant-derived compounds or polyphenols against amoebic trophozoites, most studies have been confined to general viability assays, with limited examination of specific virulence-associated gene regulation and underlying mechanistic pathways (Bharti et al. 2018; Martínez-Castillo et al. 2018). This constitutes a notable gap in the extant literature, particularly regarding the linkage between natural compounds and the molecular attenuation of pathogenicity. Accordingly, the present study aims to assess the *in vitro* anti-amoebic activity of PS against *E. histolytica*, with a specific focus on its effects on key virulence genes, including the Gal/GalNAc lectin complex and cysteine proteases (*EhCP1* and *EhCP5*). This investigation endeavors to elucidate the mechanistic basis by which PS may disrupt parasite adhesion and tissue invasion, thereby exploring its potential as a novel natural agent targeting virulence pathways in amoebiasis.

Materials and Methods

Chemicals

PS ($C_{16}H_{16}O_3$, Figure 1) purity >97%, Cell Proliferation Reagent WST-1 suitable, bovine serum, Fetal Bovine Serum (FBS), Dulbecco's Modified Eagle Medium (DMEM), dimethyl sulfoxide (DMSO), penicillin and streptomycin were procured from Sigma-Aldrich, USA.

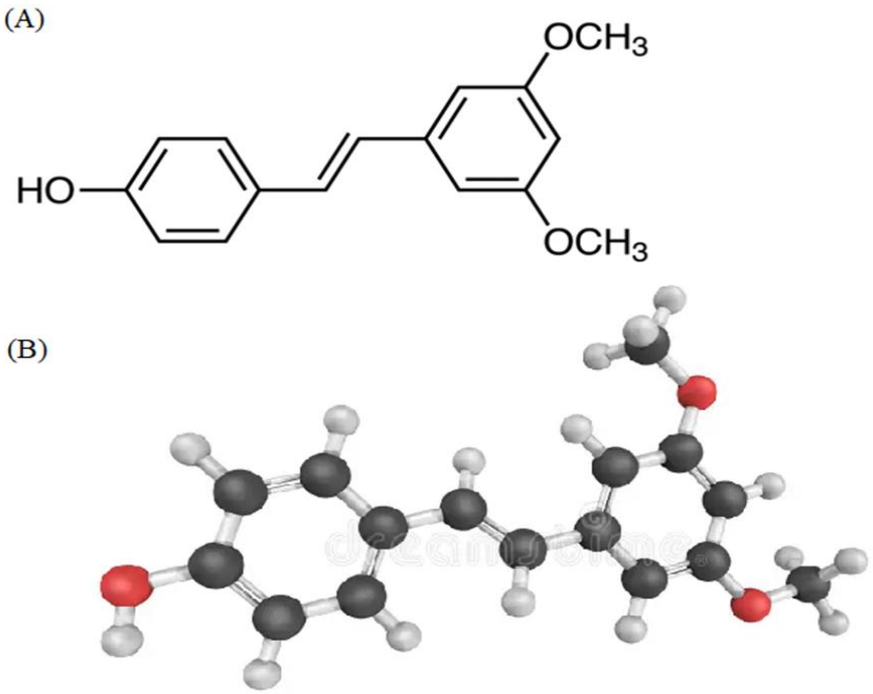

Figure 1. Chemical (A) and 3D (B) structure of pterostilbene

Parasite strain

E. histolytica HM-1: IMSS trophozoites were maintained under axenic conditions at 37°C using TYI-S-33 medium enriched with 10% bovine serum. After 48 hr. of incubation, corresponding to the late logarithmic phase of growth, the cultures were cooled to 4°C to facilitate trophozoite detachment and collection. The harvested cells were then pelleted by centrifugation at 300 × g for 5 min, concentrated, and promptly utilized for subsequent experimental procedures.

Cell culture

The FHC cell line, derived from the large intestine of a healthy donor, was obtained from the American Type Culture Collection (ATCC, CRL-1831). Cells were

cultured in DMEM medium improved with 10% FBS and 1% antibiotic solution comprising penicillin (10,000 U/mL) and streptomycin (10 mg/mL). The cultures were maintained at 37°C in a humidified atmosphere containing 5% CO_2 to ensure optimal cellular growth conditions.

Cell viability assay on *E. histolytica* trophozoites

To evaluate the impact of PS on the viability of *E. histolytica* trophozoites, the tetrazolium-based WST-1 assay was utilized as an indicator of cell viability. For the experimental procedure, 2×10^4 trophozoites were seeded into each well of a 96-well plate containing 200 µL of sterile TYI-S-33 medium. The cells were then exposed for 24 hr to varying concentrations of PS and MZ (Sanofi, México) ranging from 10 to 200 µM, as well as the combination of MZ + PS (at IC_{50} concentration). To evaluate the interaction between PS and MZ, each compound was first tested individually to determine its IC_{50} against *E. histolytica* trophozoites. The individual IC_{50} values were 37.1 µM for PS and 28.6 µM for MZ. Subsequently, PS (2.5-100 µM) and MZ (2.5-100 µM) were evaluated in combination, and the inhibitory effect of the combined treatment was used to determine the corresponding combination IC_{50}. Trophozoites maintained in complete TYI-S-33 medium supplemented with DMSO served as the negative control. Post-incubation, the culture supernatant was carefully removed, and the trophozoites were washed three times with phosphate-buffered saline (PBS). Subsequently, the WST-1 reagent was prepared by mixing 95 µL of PBS with 5 µL of WST-1 solution, and 100 µL of this mixture was added to each well. The plates were incubated in the dark at 37°C for 30 min. Following incubation, 50 µL of the supernatant from each well was transferred to a fresh 96-well plate and absorbance was measured at 450 nm using an ELISA plate reader. Data are presented as mean values ± standard deviation. The half-maximal inhibitory concentration (IC_{50}) values were calculated using the Probit statistical analysis (Cruz-Baquero et al. 2023).

Assessment of combined drug interactions

To further characterize the interaction between PS and MZ when administered simultaneously, the fractional inhibitory concentration (FIC) index for each drug was determined by dividing its IC_{50} value in the combination assay by its IC_{50} value when tested individually (Masoori et al. 2024). The overall interaction was quantified by calculating the sum of the FIC indices (ΣFIC). Interactions were categorized as "synergistic" if ΣFIC was less than or equal to 0.5, "additive" if ΣFIC ranged from 0.5 to 1.0, and "indifferent" if ΣFIC was greater than 1.0 but less than or equal to 4.0 (Odds 2003). The interaction between PS and MZ was preliminarily interpreted using the FICI, a widely recognized approach for assessing synergistic effects in antimicrobial and antiparasitic drug combinations.

Cell cytotoxicity assay

Approximately 1×10^4 FHC cells were seeded into each well of 96-well culture plates and allowed to adhere before treatment. Cells were subsequently exposed to different concentrations of PS and MZ for 24 hr. The concentration range used for each compound was identical to that employed in the corresponding dose–response experiments. For the combination treatment, PS and MZ were applied simultaneously at the concentrations specified for the combination assay. A vehicle control containing the corresponding concentration of DMSO without PS or MZ (100, 200, 300, and 400 µM) was included. The final volume in each well was adjusted to 200 µL. For the viability assay, 95 µL of PBS was combined with 5 µL of WST-1 reagent and added to 100 µL of the treated cell suspension in each well. Following incubation at 37°C for 30 min in the dark, 50 µL of the resulting

supernatant was carefully transferred to a fresh 96-well plate. Absorbance was then recorded at 450 nm using an ELISA plate reader. Cell viability was expressed as a percentage relative to untreated control cells, and a dose-response curve was constructed to determine the half-maximal cytotoxic concentration (CC_{50}) of the compound (Cruz-Baquero et al. 2023; Cheraghipour et al. 2024; Mahmoudvand et al. 2016). The selectivity index (SI) was computed to assess the specificity of the evaluated compounds for *Entamoeba* parasites in comparison to host cells. The SI values were derived using the following equation:

SI = CC_{50} (FHC cells) / IC_{50} (trophozoites),

Elevated SI values reflect increased selectivity toward the parasites alongside reduced cytotoxicity to host cells (Mahmoudvand et al. 2022).

Adhesion assay

The influence of PS on the adhesive capacity of *E. histolytica* trophozoites was assessed through a monolayer adhesion assay (Petri et al. 1987). In brief, trophozoites in the logarithmic phase of growth were treated with sublethal concentrations of PS (IC_{50}), MZ (IC_{50}), and PS+MZ both in IC_{50} concentrations for 24 hr at 37°C. Post-treatment, trophozoites were collected by incubation on ice, washed twice with PBS (pH 7.2), and adjusted to a concentration of 1×10^5 cells/mL. FHC cell lines were cultured in 24-well plates until a confluent monolayer was established. Subsequently, both treated and untreated trophozoites were introduced to the epithelial monolayers and incubated at 37°C for 60 min under standard culture conditions. Following incubation, non-adherent trophozoites were removed by gently washing the wells three times with PBS. The adherent trophozoites were then detached by chilling the plates on ice and quantified using a hemocytometer under light microscopy. The adhesion percentage was determined by comparing the number of adherent trophozoites to the initial number of trophozoites added per well. All assays were conducted in triplicate. Data are presented as mean ± standard deviation (SD) and were statistically compared to the untreated control group.

Intracellular reactive oxygen species (ROS) assay

The generation of intracellular ROS in *E. histolytica* trophozoites following treatment with PS (IC_{50}), MZ (IC_{50}), and PS+MS both in IC_{50} concentrations was assessed utilizing the fluorescent probe 2′,7′-dichlorofluorescin diacetate (DCFH-DA). In brief, trophozoites were seeded into 96-well plates at a density of 1×10^5 cells per well and subjected to varying concentrations of PS for 24 hr at 37°C. Untreated trophozoites served as the negative control, whereas menadione (25 µM, Sigma-Aldrich, USA) was employed as the positive control. Post-treatment, the trophozoites were washed twice with PBS and incubated with DCFH-DA at a final concentration of 10 µM in the dark at 37°C for 30 min. Excess probe was subsequently removed by washing the cells with PBS. Fluorescence intensity was quantified using a microplate reader with excitation and emission wavelengths set at 485 nm and 530 nm, respectively. Intracellular ROS levels were expressed as relative fluorescence intensity normalized to the untreated control group. All experiments were conducted in triplicate, and results are presented as mean ± standard deviation. An increase in fluorescence intensity was interpreted as an elevation in intracellular ROS production induced by PS treatment (Wang and Joseph 1999).

Assessment of the expression gene level of virulence factors

E. histolytica trophozoites (2×10^4) were initially treated with PS or MZ individually at their respective IC_{50} concentrations, as well as with combined treatments of PS or MZ, each at their IC_{50} values, for a period of 48 hr.

RNA extraction

Total RNA was isolated from collected specimens using a silica membrane-based commercial extraction kit (Qiagen, Germany). The procedure was conducted in full compliance with the manufacturer's recommendations to preserve RNA quality and yield. Quantification of the extracted RNA was performed using a Nanodrop spectrophotometer, whereas sample purity was determined from the absorbance ratios at 260/280 nm and 260/230 nm. To prevent contamination by genomic DNA during downstream analyses, RNA preparations were treated with RNase-free DNase I (Fermentas, USA).

Reverse transcription

First-strand complementary DNA (cDNA) was generated from purified RNA using a Qiagen reverse transcription kit and a programmable thermal cycler. The synthesis protocol was carried out according to the supplier's instructions to ensure efficient conversion of RNA templates into cDNA suitable for quantitative gene expression analysis.

Primer validation and design

Specific primer sets targeting *EhCP1*, *EhCP5*, *Gal/GalNAc lectin (hgl)*, and the housekeeping gene Actin (*EhActin*) were designed and are listed in Table 1 (Olivos-García et al. 2020; Thibeaux et al. 2013). Primer specificity and amplification performance were assessed during assay validation. Amplification efficiencies were determined using standard curves generated from a five-step serial dilution series (1:5) of pooled cDNA and were within the recommended range of 90–110%. Amplicon specificity was assessed by melting-curve analysis which showed a single distinct peak for each target. The stability of *EhActin* expression was evaluated across the experimental groups and showed minimal variation. Three independent biological replicates were analyzed, with each biological sample evaluated in duplicate technical reactions (Supplementary Table S1).

Table 1. Characteristics of the virulence-related genes and primer sequences used for quantitative real-time PCR in *Entamoeba histolytica*.

Primer	***Sequence (5'–3')***	***Size (bp)***
EhCP1	*F: TGGGAGTTGATGTTGATGGC* *R: CCTTCTTGTTGTTGCCCTTG*	*125*
EhCP5	*F: TGGTGGTGTTCAAGGATGAG* *R: CAGCATAGGTTGTTGGTGGT*	*120*
hgl	*F: GCTGTTGTTGCTGTTGCTGT* *R: AGTTGTTGCGGTTGATGGTT*	*136*
EhActin	*F: TGTTCCAATCTATGAGGGATACAC* *R: TTGAAGGTAGTTTCGTGGATGC*	*142*

Quantitative real-time PCR

Relative transcription levels of the selected inflammatory genes were quantified using SYBR Green-based real-time PCR. Each reaction was prepared in a final volume of 20 µL containing cDNA template, gene-specific primers, and SYBR Green Master Mix (Qiagen, Germany). *β-actin* served as the internal normalization control. Thermal cycling conditions consisted of an initial denaturation step at 95°C for 8 min, followed by 40 amplification cycles comprising denaturation at 95°C for 10 sec, annealing at 60°C for 10 sec, and extension at 73°C for 5 sec. A final extension step was performed at 75°C for 1 min. At the conclusion of each run, melting-curve analysis was conducted to verify amplification specificity and exclude primer-dimer formation. Relative gene expression was calculated using the $2^{-\Delta\Delta Ct}$ method, with results expressed as fold changes relative to the non-treated control group (Control group expression was set to 1.0.). Data processing and Ct value analysis

were carried out using the Bio-Rad iQ5 Optical System software. All assays included three independent biological replicates, with each sample analyzed in duplicate technical replicates. Consistent *β-actin* expression was observed across all experimental groups, supporting its use as the normalization gene. Both intra-assay and inter-assay variability remained below 10% for all investigated transcripts, demonstrating the reliability and reproducibility of the RT-qPCR measurements.

Statistical analysis

All experiments were performed using three independent biological replicates unless otherwise stated by means of SPSS software Version 26.0. For assays involving technical replication, each biological sample was measured in the indicated number of technical replicates, and technical replicates were averaged before statistical analysis. For RT-qPCR, three independent biological samples were analyzed, with each sample assessed in duplicate technical reactions. Statistical analyses were performed using the biological replicate values rather than treating technical replicates as independent observations. Results are presented as mean ± standard deviation (SD). Differences among treatment groups were evaluated using one-way analysis of variance (ANOVA), followed by Tukey's multiple-comparison test. A p value <0.05 was considered statistically significant.

Results

E. histolytica trophozoite viability

In WST-1 assay, treatment with PS resulted in a significant, dose-dependent reduction in the viability of *E. histolytica* trophozoite (Figure 2A). Furthermore, the concurrent administration of MZ and PS exhibited a more pronounced inhibitory effect on the viability of *E. histolytica* trophozoite compared to the effects observed with either compound alone ($p<0.001$). The calculated IC_{50} values for PS, MZ, and the combined MZ+PS treatment were 37.1, 28.6, and 12.7 µM, respectively.

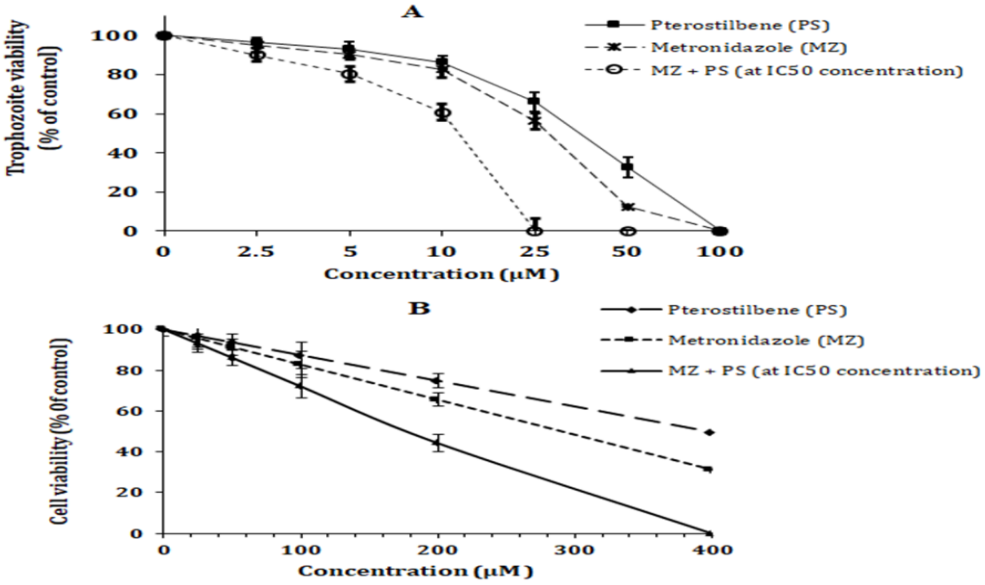

Figure 2. Anti-amoebic (A) and cytotoxicity (B) activity of pterostilbene (PS), metronidazole (MZ), and their combination against *Entamoeba histolytica* trophozoites and in FHC cells. Trophozoite viability was assessed using the WST-1 assay following 24 hr. of treatment PS and MZ reduced parasite viability in a dose-dependent manner, while the combination treatment exhibited significantly greater inhibitory activity compared with either monotherapy. Data are presented as mean ± SD of three independent experiments (N=3).

Synergistic interaction between PS and MZ

Evaluation of the synergistic interaction demonstrated that the combination of PS and MZ yielded FICI values of 0.342 for PS and 0.444 for MZ. Both values fall below the established threshold for synergy, indicating a strong cooperative interaction between these two agents.

Cytotoxic effects and SI

As illustrated in Figure 2B, treatment of FHC cells with PS, MZ, and their combination induced a dose-dependent reduction in cell viability, as measured by the WST-1 assay. The CC_{50} values were determined to be 397.6 µM for PS, 291.2 µM for MZ, and 179.6 µM for the combined treatment. Additionally, the SI values were calculated as 10.71 for PS, 10.18 for MZ, and 14.14 for the combination. Notably, the PS–MZ combination exhibited the lowest CC_{50} and the highest SI values among the treatments evaluated.

Effect on the adhesion of *E. histolytica* trophozoites

The administration of PS led to a statistically significant decrease in the adhesion capacity of *E. histolytica* trophozoites relative to the untreated control group ($p<0.01$). Specifically, the percentage of adhered trophozoites declined from 70.1 ± 4.33% in the control group to 44.6 ± 2.86% following PS treatment. Notably, the combined application of MZ and PS produced the most pronounced inhibitory effect on parasite adhesion, reducing the adhesion rate to 22.7 ± 2.13%, which was significantly lower than the reductions observed with either agent alone ($p<0.001$) (Figure 3).

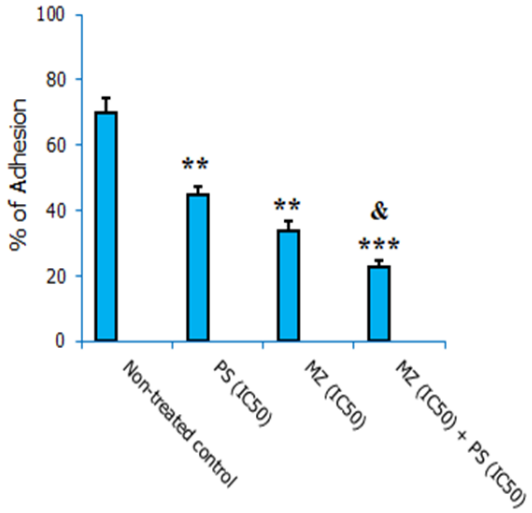

Figure 3. Effect of pterostilbene (PS), metronidazole (MZ), and their combination on the adhesion capacity of *Entamoeba histolytica* trophozoites. Adhesion ability was assessed after 24 hr of treatment and is expressed as the percentage of adherent trophozoites relative to the total cell population. The combination treatment produced the greatest reduction in parasite adhesion compared with either agent alone. Results are shown as mean ± SD of three independent experiments. Statistical significance was evaluated using one-way ANOVA followed by Tukey's post hoc test (**$p<0.01$ and ***$p<0.001$ versus control; &$p<0.05$ versus monotherapy groups).

Effect on intracellular ROS generation

ROS levels were measured using the DCFH-DA fluorescence assay following treatment with PS, MZ, and their combination. As depicted in Figure 4, treatment with PS induced a statistically significant increase in ROS production in trophozoites compared to the untreated control group ($p<0.05$), corresponding to a 1.79-fold rise in fluorescence intensity. Notably, trophozoites exposed to the combined treatment exhibited the highest intracellular ROS accumulation, with a 3.62-fold increase relative to control values, which was significantly greater than the increases observed with either PS or MZ alone ($p<0.05$).

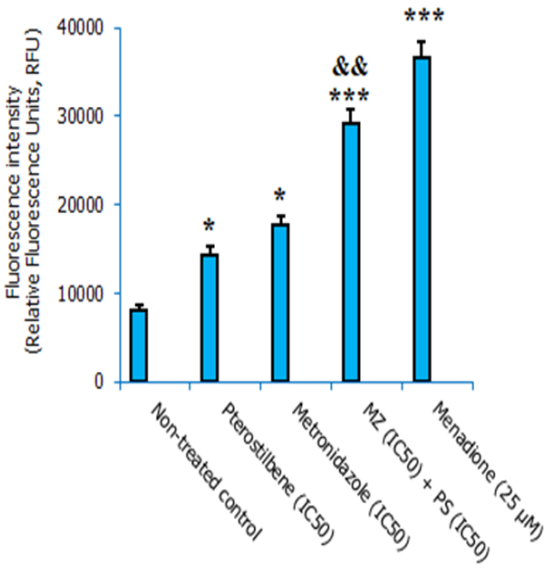

Figure 4. Effect of pterostilbene (PS), metronidazole (MZ), and their combination on intracellular reactive oxygen species (ROS) generation in *Entamoeba histolytica trophozoites*. Intracellular ROS levels were quantified using the DCFH-DA fluorescence assay following 24 hr. of treatment. Results are expressed as relative fluorescence intensity (RFU) and presented as mean ± SD from three independent experiments. Statistical significance was determined by one-way ANOVA followed by Tukey's post hoc test (*p<0.05 and ***p<0.001 versus control; &&p<0.05 versus monotherapy groups).

Effect on the expression of virulence genes

The administration of PS markedly influenced the expression patterns of virulence-associated genes in *E. histolytica*. As depicted in Figure 5, the relative mRNA levels of *EhCP1*, *EhCP5*, and *hgl* were significantly downregulated following PS treatment in comparison to the untreated control group ($p<0.05$). Specifically, *EhCP1* expression was reduced to 0.46-fold, while *EhCP5* expression decreased to 0.34-fold in the PS-treated samples. Similarly, *hgl* expression showed a significant reduction to 0.42-fold relative to controls. Notably, the combined treatment with PS and MZ elicited the most substantial inhibitory effect, exhibiting a synergistic downregulation across all evaluated virulence genes. In this group, *EhCP1* expression declined to 0.21-fold, *EhCP5* to 0.16-fold, and *hgl* to 0.19-fold, all of which were significantly lower than the levels observed with either monotherapy alone ($p<0.05$).

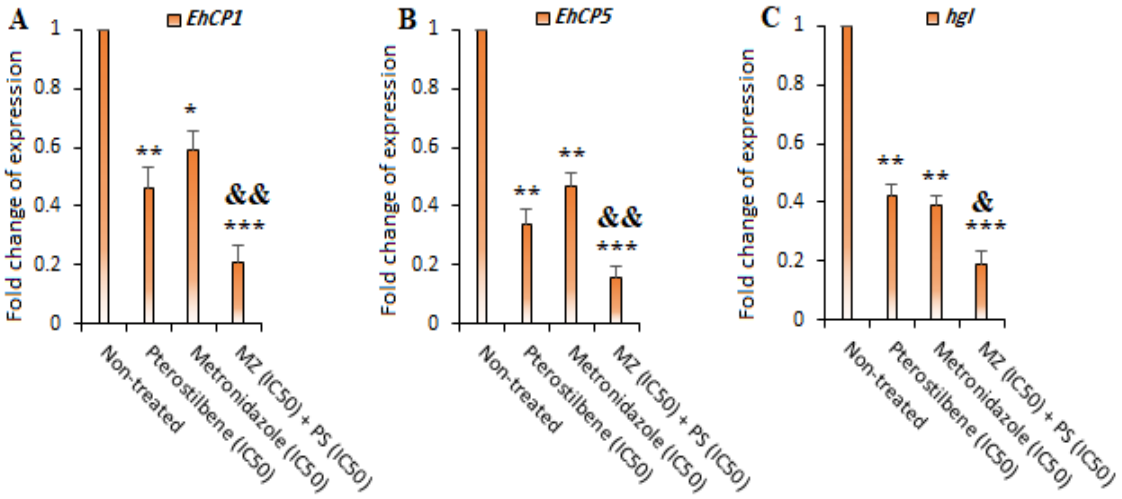

Figure 5. Effect of pterostilbene (PS), metronidazole (MZ), and their combination on the expression of virulence-associated genes in *Entamoeba histolytica* trophozoites. Relative mRNA expression levels of (A) *EhCP1*, (B) *EhCP5*, and (C) *hgl* were determined by quantitative real-time PCR following 48 hr of treatment. Gene expression levels were normalized to the housekeeping gene *EhActin* and calculated using the $2^{-\Delta\Delta Ct}$ method. Data are presented as mean ± SD from three independent experiments. Statistical significance was analyzed by one-way ANOVA followed by Tukey's post hoc test (*p<0.05, **p<0.01 and ***p<0.001 versus control; &p<0.05 and &&p<0.01 versus monotherapy groups).

Discussion

Despite the widespread use of metronidazole for amoebiasis, treatment-related limitations have encouraged the search for alternative or adjunctive anti-amoebic agents (Danish et al. 2023; Nasrallah et al. 2022). PS, a bioactive stilbene with well-documented antimicrobial and anti-inflammatory properties, has recently attracted attention as a potential antiparasitic compound. However, its activity against *E. histolytica* has not been previously investigated. Therefore, the present study aimed to address this important gap by evaluating the anti-amoebic efficacy of PS alone and in combination with MZ.

In the current investigation, PS demonstrated significant anti-amoebic activity against *E. histolytica* trophozoites and notably augmented the therapeutic efficacy of MZ when administered concomitantly. This observed synergistic interaction is of particular importance, as combination therapy is increasingly acknowledged as an effective approach to enhance antiparasitic outcomes, mitigate drug-associated toxicity, and potentially delay the development of resistance. The capacity of PS to potentiate MZ activity implies that these compounds may act upon distinct yet complementary biological pathways within the parasite. Although data concerning the anti-protozoal effects of PS remain limited, several studies have substantiated its potential as an antiparasitic agent (Mahmoudvand et al. 2011). For instance, Ferreira et al. (2011) assessed PS alongside other resveratrol analogues against *Leishmania amazonensis* using both promastigote and intracellular amastigote models, revealing that PS exerted pronounced leishmanicidal effects while exhibiting relatively low cytotoxicity toward host macrophages. The authors posited that the physicochemical properties of PS, particularly its enhanced lipophilicity relative to resveratrol, may facilitate cellular uptake and thereby improve antiparasitic efficacy. These findings align with the anti-amoebic activity documented in the present study and suggest that PS antiparasitic properties may extend across diverse protozoan species.

The biological activity of PS may be partially attributed to its structural features. Compared to resveratrol, PS exhibits increased membrane permeability, greater metabolic stability, and superior bioavailability, characteristics that likely promote intracellular accumulation and interaction with critical parasitic targets. Prior research on stilbene-derived compounds has demonstrated their capacity to disrupt cellular homeostasis, interfere with energy metabolism, alter membrane function, and induce oxidative stress in protozoan parasites (Ferreira et al. 2015; Ferreira et al. 2014). Although the precise mechanisms underlying the anti-amoebic effects observed herein remain to be fully elucidated, existing evidence suggests that PS may influence multiple pathways essential for trophozoite survival and proliferation. An additional salient finding of this study was the synergistic interaction between PS and MZ. Comparable advantages of combination therapy have been reported in various parasitic diseases, wherein concurrent targeting of distinct cellular processes yielded enhanced antiparasitic efficacy relative to monotherapy (Mutiso et al. 2011). Such synergistic interactions are particularly advantageous in the context of amoebiasis, as reducing MZ dosage may diminish adverse effects and improve patient adherence.

In addition to its direct anti-amoebic effects, PS significantly increased intracellular ROS levels in *E. histolytica* trophozoites, with the combined treatment producing the most pronounced oxidative response. Oxidative stress is known to influence parasite survival and virulence, and disruption of redox homeostasis has been proposed as a potential strategy for antiparasitic intervention (Pineda and Perdomo 2017; Rastew et al. 2012; Guillén

2023). In the present study, the increased ROS levels following PS treatment were associated with reduced trophozoite viability; however, the present experimental design does not establish a direct causal relationship between ROS generation and the anti-amoebic effect of PS. Therefore, the observed increase in intracellular ROS should be considered a potential contributor to, rather than definitive evidence of, the biological activity of PS. Further studies using ROS scavengers or antioxidant rescue experiments will be required to determine whether oxidative stress is causally involved in PS-mediated parasite killing.

Beyond its impact on trophozoite viability, PS markedly downregulated the expression of critical virulence-associated genes, including *EhCP1*, *EhCP5*, and *hgl*. Cysteine proteases are recognized as principal virulence factors in *E. histolytica*, playing essential roles in tissue invasion, degradation of the extracellular matrix, immune evasion, and host cell destruction (Moncada et al. 2006; Siqueira-Neto et al. 2013; Guillén et al. 2012). Notably, *EhCP5* has been extensively characterized as a major pathogenic determinant, with prior studies demonstrating a strong correlation between its expression and parasite virulence (Moncada et al. 2006; Siqueira-Neto et al. 2013). Therefore, the observed suppression of *EhCP1* and *EhCP5* suggests that PS may attenuate the parasite's invasive capacity in addition to diminishing trophozoite survival. The heavy subunit of the *hgl* is another well-established virulence factor that facilitates trophozoite adherence to intestinal epithelial cells and components of the extracellular matrix (Petri et al. 2002; Singh et al. 2024). Given that adhesion is a prerequisite for colonization, cytotoxicity, and tissue invasion, disruption of lectin-mediated attachment has long been regarded as a viable anti-virulence strategy (Petri et al. 2002; Singh et al. 2024). Consistent with this notion, the transcriptional downregulation of *hgl* observed in this study was accompanied by a significant reduction in trophozoite adhesion, indicating a functional link between decreased expression of this adhesin and impaired parasite attachment. Prominently, the combination of PS and MZ consistently exerted the most potent inhibitory effects on ROS homeostasis, virulence gene expression, and trophozoite adhesion. These results suggest that the synergistic interaction between these agents extends beyond mere parasite eradication, potentially targeting molecular pathways integral to parasite pathogenicity.

The safety profile of prospective anti-amoebic agents represents a crucial consideration in the drug development process. In the present study, PS, administered both as a monotherapy and in combination with MZ, exhibited reduced cytotoxic effects on normal FHC cells relative to its activity against *E. histolytica* trophozoites, thereby demonstrating a favorable selectivity index. Notably, the selectivity indices obtained across all treatment regimens fell within the range conventionally regarded as indicative of promising antiparasitic drug candidates (Katsuno et al. 2015). The selectivity index is a key parameter for assessing the therapeutic potential of novel antiparasitic compounds, as it reflects their preferential cytotoxicity toward parasitic cells compared to host cells (Katsuno et al. 2015; Peña-Morán et al. 2016). The advantageous selectivity profile observed in this investigation suggests that the anti-amoebic activity of PS is unlikely to result from nonspecific cytotoxic effects. Furthermore, although combination therapy enhanced antiparasitic efficacy, it maintained an acceptable safety margin and exhibited the highest selectivity among the evaluated treatments. These findings are consistent with previous studies reporting the relatively low toxicity and favorable safety characteristics of PS in mammalian cell models (McCormack and McFadden 2013; Kapetanovic et al. 2011). Collectively, the current results indicate that PS possesses both potent anti-amoebic activity and a

desirable selectivity profile, thereby justifying further exploration of its potential as an adjunctive agent in the management of amoebiasis.

The present study has several limitations that should be acknowledged. First, all experiments were conducted under *in vitro* conditions; therefore, the observed anti-amoebic effects may not fully reflect the complexity of host–parasite interactions in vivo. Second, although the results suggest that oxidative stress and suppression of virulence-associated genes contribute to the activity of PS, the precise molecular mechanisms underlying these effects remain to be elucidated. Additionally, only a limited number of virulence markers were investigated, and other pathways potentially involved in parasite survival and pathogenicity were not assessed. Despite these limitations, the findings provide the first evidence of the anti-amoebic and anti-virulence activities of PS against *E. histolytica*. Future studies should evaluate the efficacy and safety of PS in experimental models of amoebiasis, investigate its pharmacokinetic and pharmacodynamic properties, and further characterize the molecular pathways involved in its antiparasitic action. Moreover, given the promising synergistic interaction observed with MZ, additional studies are warranted to optimize combination regimens and explore their potential to improve therapeutic outcomes while reducing drug-associated toxicity.

PS exhibits significant anti-amoebic activity against *E. histolytica* and enhances the activity of MZ under the experimental conditions investigated. These effects were accompanied by increased intracellular ROS levels, downregulation of virulence-associated gene expression, and reduced parasite adhesion. However, the present findings demonstrate associations rather than definitive causal mechanisms. Therefore, further mechanistic and in vivo studies are warranted to determine the contribution of oxidative stress and virulence-related pathways to the anti-amoebic activity of PS.

Acknowledgment

The author thanks the staff of parasitological laboratory of Biology Department, Education college, Al-Qadisiyah University.

Conflicts of interest

The author hereby declares that there are no conflicts of interest associated with this study.

Authors' Contributions

HSA contributed to the conceptualization, methodology, investigation, formal analysis, original draft writing, as well as the review and editing of the manuscript.

Abbreviations

FICI: fractional inhibitory concentration index
ROS: reactive oxygen species
PS: pterostilbene
MZ: metronidazole
IC_{50}: half-maximal inhibitory concentration
CC_{50}: half-maximal cytotoxic concentration
SI: selectivity index

References

Alnomasy S, Al-Awsi GR, Raziani Y, Albalawi AE, Alanazi AD, Niazi M (2021) Systematic review on medicinal plants used for the treatment of Giardia infection. Saudi J Biol Sci 28(9):5391-402.

Bharti N, Mohapatra PP, Singh S (2018) Plant-based antiamoebic natural products: literature review and recent developments. In: Front Nat Prod Chem 4: 1-40.

Chaachouay N, Zidane L (2024) Plant-derived natural products: a source for drug discovery and development. Drugs Drug Candidates 3(1):184–207.

Cheraghipour K, Khalaf AK, Moradpour K, Zivdari M, Beiranvand M, Shakib P (2023) Synthesis, characterization, and antiparasitic effects of zinc oxide nanoparticles-eugenol nanosuspension against Toxoplasma gondii infection. Heliyon 9(8):e.

Cruz-Baquero A, Téllez-Valencia A, Reséndiz-Albor AA (2023) In vitro evaluation of the antiamoebic activity of kaempferol against trophozoites of Entamoeba histolytica and in the interactions of amoebae with hamster neutrophils. Int J Mol Sci 24(13):11216.

Danish W, Bibi A, Suleman A, Naveed F, Fuzail MM, Mehmood M, Imran M (2023) Amoebiasis in one health perspective. In: One Health Triad, Unique Scientific Publishers, Faisalabad, Pakistan, vol 3, pp 146–150.

Estrela JM, Ortega A, Mena S, Rodriguez ML, Asensi M (2013) Pterostilbene: biomedical applications. Crit Rev Clin Lab Sci 50(3):65–78.

Ferreira C, Soares DC, Nascimento MTC (2014) Resveratrol is active against Leishmania amazonensis: in vitro effect of its association with amphotericin B. Antimicrob Agents Chemother 58(10):6197–6208.

Ferreira C, Soares DC, Saraiva EM (2015) Leishmanicidal effect of synthetic trans-resveratrol analogs. PLoS One 10(10):e0141778.

Guillén N (2023) Pathogenicity and virulence of Entamoeba histolytica, the agent of amoebiasis. Virulence 14(1):2158656.

Guillén N & Avila EE (2012) Virulence and virulence factors in Entamoeba histolytica, the agent of human amoebiasis. Microbes Infect 14(15):1428–1441.

Kapetanovic IM, Muzzio M, Huang Z, Thompson TN, McCormick DL (2011) Pharmacokinetics, oral bioavailability, and metabolic profile of pterostilbene in rats. Cancer Chemother Pharmacol 68(3):593–601.

Katsuno K, Burrows JN, Duncan K, van Huijsduijnen RH, Kaneko T, Kita K (2015) Hit and lead criteria in drug discovery for infectious diseases of the developing world. Nat Rev Drug Discov 14(11):751–758.

Kosuru R, Rai U, Prakash S, Singh A, Singh S (2016) Promising therapeutic potential of pterostilbene and its mechanistic insight based on preclinical evidence. Eur J Pharmacol 789:229–243.

Mahmoudvand H, Mohebali M, Sharifi I, Keshavarz H, Hajjaran H, Akhoundi B (2011) Epidemiological aspects of visceral leishmaniasis in Baft district, Kerman Province, Southeast of Iran. Iran J Parasitol 6(1):1.

Mahmoudvand H, Sepahvand P, Jahanbakhsh S, Azadpour M. (2016) Evaluation of the antileishmanial and cytotoxic effects of various extracts of garlic (*Allium sativum*) on Leishmania tropica. J Parasit Dis 40(2):423-6.

Mahmoudvand H, Yadegari JG, Khalaf AK, Hashemi MJ, Dastyarhaghighi S, Salimikia I (2022) Chemical composition, antileishmanial, and cytotoxic effects Ferula macrecolea essential oil against Leishmania tropica. Parasite Epidemiol Control 19:e00270.

Martínez-Castillo M, Pacheco-Yepez J, Flores-Huerta N, Guzmán-Téllez P, Jarillo-Luna RA, Cárdenas-Jaramillo LM, Campos-Rodríguez R, Shibayama M (2018) Flavonoids as a natural treatment against Entamoeba histolytica. Front Cell Infect Microbiol 8:209.

Masoori L, Khalaf AK, Ezzatkhah F, Balaña-Fouce R, Mahmoudvand H (2024) Promising effects of 1,8-cineole to control Giardia lamblia infection: targeting the inflammation, oxidative stress, and infectivity. Acta Trop 255:107201.

McCormack D & McFadden D (2013) A review of pterostilbene antioxidant activity and disease modification. Oxid Med Cell Longev 2013:575482.

Moncada D, Keller K, Ankri S (2006) Increased expression of the major cysteine proteinases by stable episomal transfection underlines the important role of EhCP5 for the pathogenicity of *Entamoeba histolytica*. Mol Biochem Parasitol 149(1):58–64.

Morán P, Serrano-Vázquez A, Rojas-Velázquez L, González E, Pérez-Juárez H, Hernández EG, Padilla MD, Zaragoza ME, Portillo-Bobadilla T, Ramiro M, Ximénez C (2023) Amoebiasis: advances in diagnosis, treatment, immunology features and the interaction with the intestinal ecosystem. Int J Mol Sci 24(14):11755.

Mutiso JM, Macharia JC, Barasa M, Taracha E, Bourdichon AJ, Gicheru MM (2011) In vitro and in vivo antileishmanial efficacy of a combination therapy of diminazene and artesunate against Leishmania donovani. Parasitol Res 109:1427–1433.

Nasrallah J, Akhoundi M, Haouchine D, Marteau A, Mantelet S, Wind P, Benamouzig R, Bouchaud O, Dhote R, Izri A (2022) Updates on the worldwide burden of amoebiasis: a case series and literature

review. J Infect Public Health 15(10):1134–1141.

Obrador E, Salvador-Palmer R, Jihad-Jebbar A, López-Blanch R, Dellinger TH, Dellinger RW, Estrela JM (2021) Pterostilbene in cancer therapy. Antioxidants (Basel) 10(3):492.

Odds FC (2003) Synergy, antagonism, and what the chequerboard puts between them. J Antimicrob Chemother 52(1):1.

Olivos-García A, Saavedra E, Ramos-Martínez E et al (2020) Differential pathogenic gene expression of *E. histolytica* in patients with different clinical forms of amoebiasis. Microorganisms 8(10):1556.

Peña-Morán O, Villarreal-Treviño L, de la Garza M et al (2016) In vitro susceptibility and selectivity index as criteria for evaluation of anti-parasitic compounds. Exp Parasitol 168:66–75.

Petri WA, Haque R, Mann BJ (2002) The bittersweet interface of parasite and host: lectin-mediated adherence of Entamoeba histolytica. Nat Rev Microbiol 1(1):65–73.

Petri WA, Smith RD, Schlesinger PH, Murphy CF, Ravdin JI (1987) Isolation of the galactose-binding lectin that mediates the in vitro adherence of Entamoeba histolytica. J Clin Invest 80(5):1238–1244.

Pineda E, Perdomo D (2017) Entamoeba histolytica under oxidative stress: what countermeasure mechanisms are in place? Cells 6(4):44.

Rastew E, Vicente JB, Singh U (2012) Oxidative stress resistance genes contribute to the pathogenic potential of the anaerobic protozoan parasite, Entamoeba histolytica. Int J Parasitol 42(11):1007–1015.

Samie A, ElBakri A, AbuOdeh RE (2012) Amoebiasis in the tropics: epidemiology and pathogenesis. In: Current Topics in Tropical Medicine, p 201.

Singh N, Banerjee S et al (2024) Role of various virulence factors involved in the pathogenesis of Entamoeba histolytica. Exp Parasitol 258:108841.

Siqueira-Neto JL, Debnath A, McCall LI et al (2013) Proteases from Entamoeba spp. and pathogenic free-living amoebae as virulence factors. Pathogens 2(1):118–146.

Suleiman JB, Azlan M (2025) Burden and distribution of protozoan pathogens in diarrhea cases worldwide: a systematic review and meta-analysis, 1999–2024. Cureus 17(9).

Thibeaux R, Weber C, Hon CC, Dillies MA, Avé P, Coppée JY, Labruyère E, Guillén N. (2013) Identification of the virulence landscape essential for Entamoeba histolytica invasion of the human colon. PLoS Pathog 9(12):e1003824.

Wang H &Joseph JA (1999) Quantifying cellular oxidative stress by dichlorofluorescein assay using microplate reader. Free Radic Biol Med 27(5–6):612–616.